www.cadanda.com Computer-Aided Design and Applications

Uniqueness Theorem on the Shape of Free-form Curves Defined by Three Control Points

Kenjiro T. Miura[1] , Dan Wang[2] , R.U. Gobithaasan[3] , Tadatoshi Sekine[4] and Shin Usuki[5]

[1]Shizuoka University, miura.kenjiro@shizuoka.ac.jp
[2]Shizuoka University, wang.dan.18@shizuoka.ac.jp
[3]University Malaysia Terengganu, gr@umt.edu.my
[4]Shizuoka University, sekine.tadatoshi@shizuoka.ac.jp
[5]Shizuoka University, usuki@shizuoka.ac.jp

Corresponding author: Kenjiro T. Miura, miura.kenjiro@shizuoka.ac.jp

Abstract. On the researches of free-form curves, those of the quadratic curve have been become very active because of κ-curves. In this paper, we will prove the uniqueness theorem on the shape of free-form curves defined by three control points, including non-rational: integral and rational quadratic Bézier curves, generalized trigonometric and hyperbolic curves and splines in tension.

Keywords: uniqueness theorem, quadratic curve, polynomial curve, trigonometric curve, hyperbolic curve, splines in tension
DOI: https://doi.org/10.14733/cadaps.2022.293-305

1 INTRODUCTION

On the researches of free-form curves, those of the quadratic curve have been become very active because of κ-curves[8, 7]. The κ-curve, which consists of a sequence of quadratic Bézier curves and proposed recently by [8], is an interpolating spline which is curvature-continuous almost everywhere and passes through input points at the local curvature extrema. It has been implemented as the curvature tool in Adobe Illustrator® and Photoshop® and is accepted as a favored curve design tool by many designers (see e.g. [1, 2]). We consider the reasons for the success of κ-curve to be [5]:

1. Information along contours is concentrated at local maxima of curvature.
2. Curves of low degree have smooth distribution of curvature.
3. G^2-continuous curves tend to look fairer than only G^1-continuous ones.

We emphasize especially the second reason since the curvature distribution of free-form curves defined by three control points are generally smooth.

In this paper, we will prove the uniqueness theorem on the shape of free-form curves defined by three control points, including non-rational: integral and rational quadratic Bézier curves [4], generalized trigonometric (GT) and hyperbolic (GH) curves and splines in tension [3]. For the applications of our theorem in CAD and CAGD, we might be able to select a parameterization of the curve suitable for the specific application by selecting, for example, the generalized trigonometric or the rational quadratic Bézier curves since our theorem guarantees that if the locations of their control points are the same, the shapes of these curves are identical although their blending functions are different.

2 GENERALIZED TRIGONOMETRIC BASIS

In this section, we describe our new *generalized trigonometric basis*. This is based on the trigonometric cubic Bernstein-like basis [6], which we are going to review first.

The trigonometric cubic Bernstein-like basis functions have an extra shape parameter α, and are defined by

$$\begin{aligned} f_0 &= \alpha S^2 - \alpha S + C^2 = 1 + (\alpha - 1)S^2 - \alpha S, \\ f_1 &= \alpha S(1 - S), \\ f_2 &= \alpha(S^2 + C - 1) = \alpha C(1 - C), \\ f_3 &= (1 - \alpha)S^2 - \alpha C + \alpha = 1 + (\alpha - 1)C^2 - \alpha C, \end{aligned} \tag{1}$$

where $S = \sin\frac{\pi t}{2}$, $C = \cos\frac{\pi t}{2}$, for $\alpha \in (0, 2)$, $t \in [0, 1]$. Note that these functions satisfy partition of unity, i.e., $\sum_{i=0}^{3} f_i(t) = 1$ for any α. When $\alpha = 1$, the above functions are simplified to

$$\begin{aligned} f_0 &= 1 - S, \\ f_1 &= S(1 - S), \\ f_2 &= C(1 - C), \\ f_3 &= 1 - C. \end{aligned} \tag{2}$$

If we add the second and third functions together and rename them to u, v and w, we obtain blending functions $\{u, v, w\}$ as follows:

$$\begin{aligned} u &= 1 - S, \\ v &= S(1 - S) + C(1 - C) = S + C - 1, \\ w &= 1 - C. \end{aligned} \tag{3}$$

It is straightforward to define a curve by these blending functions with three control points, which we can regard as a "linear" trigonometric curve since the highest degree the trigonometric functions are in is one.

One interesting relationship among these functions is

$$v^2 = 2uw, \tag{4}$$

which enables

$$(u + v + w)^2 = u^2 + 2uv + 4uw + 2vw + w^2, \tag{5}$$

and yields the five blending functions $\{u^2,\ 2uv,\ 4uw,\ 2vw,\ w^2\}$, associated with five control points. We can define a curve using these blending functions and regard it as a "quadratic" trigonometric curve since the highest power of each blending function is now degree two.

In a similar way, we can extend blending functions of "degree" n with $2n+1$ control points. As explained in Appendix, we can perform a recursive procedure to evaluate a curve of any degree similar to de Casteljau's algorithm avoiding the overhead of trigonometric function evaluation. We call this procedure Gobithaasan-Miura's recursive algorithm. This means that it is not necessary to calculate the coefficients of blending functions, or keep a coefficient table. The coefficients of the generalized trigonometric curve are listed as an triangle as Pascal's triangle and we call it Miura's triangle as shown in the Appendix.

3 GENERALIZED HYPERBOLIC BASIS

In this section we will derive a new basis for $\{\sinh t, \cosh t, 1\}$. Let $w(t)$ satisfy

$$\begin{aligned} w(0) &= 0 \\ w(1) &= 1 \\ \frac{dw(0)}{dt} &= 0 \end{aligned} \tag{6}$$

Hence

$$\begin{aligned} w(t) &= \frac{1}{2\sinh^2\frac{1}{2}}(\cosh t - 1) \\ &= \frac{e}{(e-1)^2}e^t(1-e^{-t})^2 \end{aligned} \tag{7}$$

We define $u(t)$ symmetric to $w(t)$ along $t = 1/2$ as $w(1-t)$

$$\begin{aligned} u(t) &= w(1-t) = \frac{1}{2\sinh^2\frac{1}{2}}(\cosh(1-t) - 1) \\ &= \frac{1}{(e-1)^2}e^{-t}(e-e^t)^2 \end{aligned} \tag{8}$$

Then

$$\begin{aligned} v(t) &= 1 - u(t) - w(t) \\ &= 1 - \frac{1}{2\sinh^2\frac{1}{2}}(\cosh t + \cosh(1-t) - 2) \\ &= \frac{(e+1)e^{-t}\left(e-e^t\right)\left(e^t-1\right)}{(e-1)^2} \end{aligned} \tag{9}$$

Figure 1 shows these basis functions.

Again fortunately we obtain the following relationship:

$$v(t)^2 = \frac{(e+1)^2}{e}u(t)w(t) \approx 5.08616u(t)w(t) \tag{10}$$

Hence for GH basis functions, $\alpha = \frac{(e+1)^2}{e} \approx 5.08616$.

Therefore we can define generalized hyperbolic basis functions as

$$\begin{aligned} \{u(t), v(t), w(t)\} = &\{\frac{1}{2\sinh^2\frac{1}{2}}(\cosh(1-t) - 1), 1 - \frac{1}{2\sinh^2\frac{1}{2}}(\cosh t + \cosh(1-t) - 2), \\ &\frac{1}{2\sinh^2\frac{1}{2}}(\cosh t - 1)\} \end{aligned} \tag{11}$$

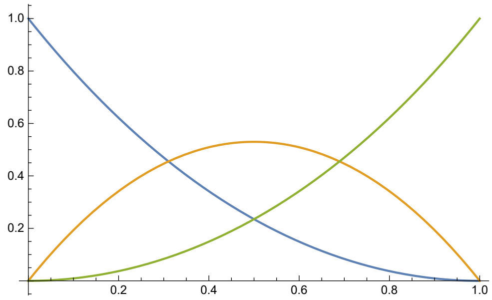

Figure 1: The linear hyperbolic basis functions

Note that the construction of the generalized hyperbolic basis is similar to that of the generalized trigonometric basis and its nice properties are inherited to the GH basis such as curve definition of any degrees, Gobithaasan-Miura's recursive algorithm and Miura's triangle.

For example, the second Miura's triangle, which is for GH basis is defined as follows: by multiplying $u(t)+v(t)+w(t)=1$ to a linear generalized hyperbolic curve,

$$\begin{aligned} \boldsymbol{C}(t) = &= u(t)^2\boldsymbol{P}_0 + 2u(t)v(t)\frac{\boldsymbol{P}_0+\boldsymbol{P}_1}{2} + (\boldsymbol{P}_0 + \frac{(e+1)^2}{e}\boldsymbol{P}_1 + \boldsymbol{P}_2)u(t)v(t) \\ &\quad +2v(t)w(t)\frac{\boldsymbol{P}_1+\boldsymbol{P}_2}{2} + w(t)^2\boldsymbol{P}_2 \\ &= u(t)^2\boldsymbol{P}_0 + 2u(t)v(t)\frac{\boldsymbol{P}_0+\boldsymbol{P}_1}{2} + \frac{e^2+4e+1}{e}\{\frac{e\boldsymbol{P}_0+(e+1)^2\boldsymbol{P}_1+e\boldsymbol{P}_2}{e^2+4e+1}\}u(t)v(t) \\ &\quad +2v(t)w(t)\frac{\boldsymbol{P}_1+\boldsymbol{P}_2}{2} + w(t)^2\boldsymbol{P}_2 \end{aligned} \tag{12}$$

where $(e\boldsymbol{P}_0+(e+1)^2\boldsymbol{P}_1+e\boldsymbol{P}_2)/e^2+4e+1 \approx 0.14112\boldsymbol{P}_0 + 0.71776\boldsymbol{P}_1 + 0.14112\boldsymbol{P}_2$.

We can construct the second Miura's triangle as follows:

$$\begin{array}{ccccccc} & & 1 & 1 & 1 & & \\ & 1 & 2 & \frac{e^2+4e+1}{e} \approx 7.08616 & 2 & 1 & \\ 1 & 3 & \frac{3(e^2+3e+1)}{e} \approx 18.2585 & \frac{e^2+4e+1}{e} \approx 11.0862 & \frac{3(e^2+3e+1)}{e} & 3 & 1 \end{array} \tag{13}$$

4 SPLINES IN TENSION

Splines in tension are functions defined piecewise to be in the space span$\{e^{\rho t}, e^{-\rho t}, 1, t\}$[3]. In this section as an extension of generalized hyperbolic basis functions, we define a new basis in the space span $\{e^{\rho t}, e^{-\rho t}, 1\}$.

Similar to Eq.(7)

$$\begin{aligned} w(t) &= \frac{1}{\cosh\rho - 1}(\cosh\rho t - 1) \\ &= \frac{\sinh^2\frac{\rho t}{2}}{\sinh^2\frac{\rho}{2}} \end{aligned} \tag{14}$$

Figure 2 shows graphs of $\{u(t), v(t), w(t)\} = \{w(1-t), 1-w(1-t)-w(t), w(t)\}$ for $\rho = 0.1$, 2 and 10. By increasing ρ, a curve defined by these basis functions approaches to a polyline connecting its control points.

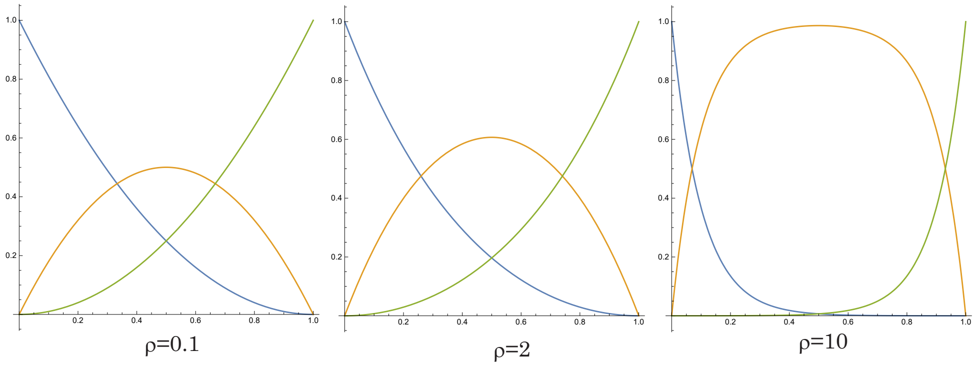

Figure 2: The linear hyperbolic basis functions in tension

For this basis, the following equation is satisfied:

$$v(t)^2 = \frac{(e^\rho + 1)^2}{e^\rho} u(t)w(t) \tag{15}$$

Note that if $\rho = 1$, $\alpha = (e+1)^2/e$ as in the previous section. If $\rho = 0$, $\alpha = 4$. In this case since the Maclaurin's expansion of $\sinh t$ is given by

$$\sinh t = t + \frac{t^3}{3!} + \frac{t^5}{5!} \cdots , \tag{16}$$

from Eq.(14) function $w(t)$ is given by

$$\begin{aligned}\lim_{\rho \to 0} w(t) &= \lim_{\rho \to 0} \frac{\sinh^2 \frac{\rho t}{2}}{\sinh^2 \frac{\rho}{2}} \\ &= \lim_{\rho \to 0} \frac{(\frac{\rho t}{2} + \frac{(\frac{\rho t}{2})^3}{3!} + \cdots)^2}{(\frac{\rho}{2} + \frac{(\frac{\rho}{2})^3}{3!} + \cdots)^2} \\ &= t^2\end{aligned} \tag{17}$$

We obtained one of the quadratic Bernstein basis functions as expected because $\alpha = 4$. Figure 3 shows $\alpha = (e^\rho + 1)^2/e^\rho$ for $0 \le \rho \le 5$. Notice that $\cosh t$ as well as $w(t)$ is an even function and the graph of α is symmetric along the y axis.

5 RATIONAL QUADRATIC BERNSTEIN BASIS

It is very common to represent a circular arc by a rational quadratic Bézier curve as

$$\boldsymbol{C}(t) = \frac{(1-t)^2 \boldsymbol{P}_0 + 2(1-t)t\sigma \boldsymbol{P}_1 + t^2 \boldsymbol{P}_2}{(1-t)^2 + 2(1-t)t\sigma + t^2} \tag{18}$$

where σ is a weight of $\boldsymbol{P}_1$. For example when $\boldsymbol{P}_0 = (-1, a)$, $\boldsymbol{P}_1 = (0, 0)$ and $\boldsymbol{P}_2 = (1, a)$ for a given a, if $\sigma = 1/\sqrt{a^2+1}$ the curve becomes a circular arc.

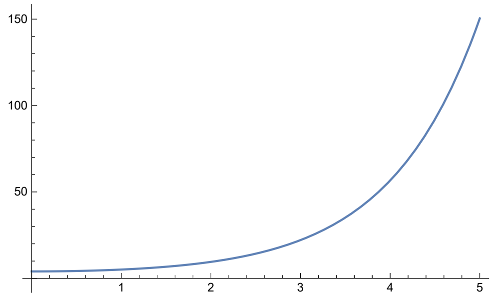

Figure 3: Function $\alpha = (e^\rho + 1)^2 / e^\rho$

Hence we define a blending function $w(t)$ as follows:

$$w(t) = \frac{t^2}{(1-t)^2 + 2(1-t)t\sigma + t^2} \tag{19}$$

For this basis, the following equation is satisfied:

$$v(t)^2 = 4\sigma^2 u(t) w(t) \tag{20}$$

Figure 4 shows graphs of $\{u(t), v(t), w(t)\} = \{w(1-t), 1 - w(1-t) - w(t), w(t)\}$ for $\sigma = 1/4$, $1/2$, $1/\sqrt{2}$, 2 and 10. By increasing σ, a curve defined by these basis functions approaches to a polyline connecting its control points.

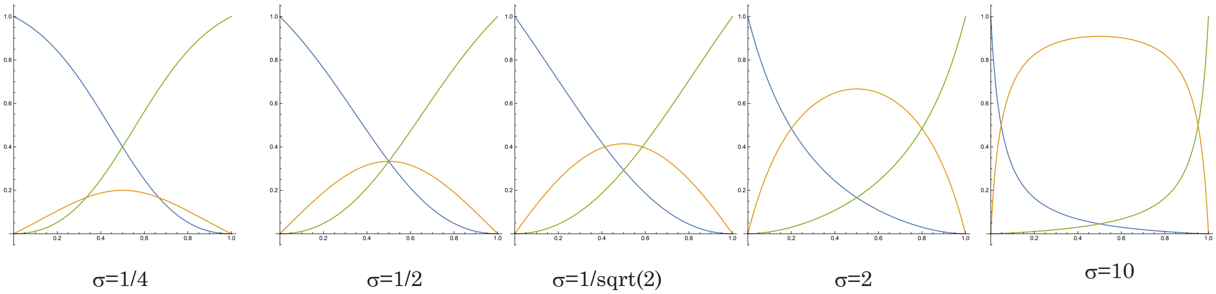

Figure 4: Rational quadratic Bernstein basis functions

Note that if $\sigma = 1$, since the basis becomes that of the non-rational quadratic Bernstein basis, $\alpha = 4$. If $\sigma = 1/\sqrt{2}$, $\alpha = 2$. However $w(t) \neq 1 - \cos(\pi t/2)$. Figure 5 compares these two basis functions and they are very similar, but not identical.

Since there are two types of the bases whose $\alpha = 2$, the conditions

$$\{1 - w(t) - w(1-t)\}^2 = \alpha w(t) w(1-t) \tag{21}$$

for a given constant $\alpha > 0$ with

$$\begin{aligned} w(0) &= 0 \\ w(1) &= 1 \\ \frac{dw(0)}{dt} &= 0 \end{aligned} \tag{22}$$

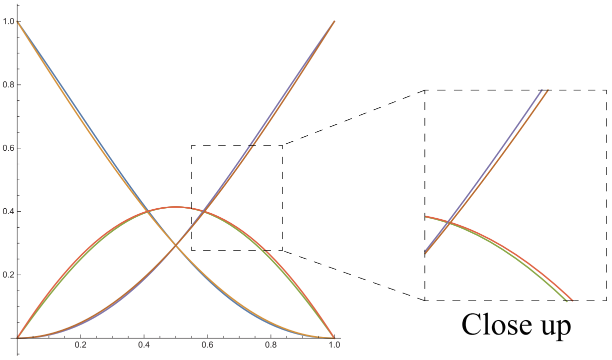

Figure 5: Comparison between the rational quadratic Bernstein basis functions (brown) and $\{1 - \sin(\pi t/2), \sin(\pi t/2) + \cos(\pi t/2) - 1, 1 - \cos(\pi t/2)\}$ (blue)

do not determine function $w(t)$ uniquely.

Notice that when $t = 1/2$, from the following equation:

$$\begin{aligned} (1 - 2w(\frac{1}{2}))^2 &= \alpha w(\frac{1}{2})^2 \\ (4-\alpha)w(\frac{1}{2})^2 - 4w(\frac{1}{2}) + 1 &= 0 \end{aligned} \tag{23}$$

When $\alpha = 4$, $w(1/2) = 1/4$. Since $0 < w(1/2) < 1$, when $\alpha < 4$, $w(1/2) = (2 - \sqrt{\alpha})/(4 - \alpha)$ and when $\alpha > 4$, $w(1/2) = (\sqrt{\alpha} - 2)/(\alpha - 4)$. Therefore although the basis functions are different, if they have the same α value, when $t = 1/2$, the values of these basis functions are exactly the same.

6 COMPARISON BETWEEN LINEAR GT BASIS AND RATIONAL QUADRATIC BERNSTEIN BASIS

We would like to know how different are the linear GT and rational quadratic Bernstein bases. When $\boldsymbol{P}_0 = (1, 0)$, $\boldsymbol{P}_1 = (1, 1)$ and $\boldsymbol{P}_2 = (0, 1)$, the linear generalized trigonometric curve with these control points becomes a quadrant or a quarter of a circular arc. For the same control points with $\sigma = 1/\sqrt{2}$, the rational quadratic Bézier curve becomes the same quadrant. As shown in Fig.6, the numerator of the curve is a non-rational quadratic Bézier curve with $\boldsymbol{P}_0 = (1, 0)$, $\boldsymbol{P}_1 = (\sigma, \sigma)$ and $\boldsymbol{P}_1 = (0, 1)$ and the denominator is the x-coordinate of a non-rational quadratic Bézier curve with $\boldsymbol{P}_0 = (1, 0)$, $\boldsymbol{P}_1 = (\sigma, 1/2)$ and $\boldsymbol{P}_2 = (1, 1)$. Hence the effect of the denominator is only a scaling factor of the coordinate of the numerator and the polar angle of the point on the quadrature is the same as the point on the non-rational quadratic Bézier curve.

The polar angle θ of the non-rational quadratic Bézier curve is given by

$$\theta = \arctan \frac{2(1-t)t\sigma + t^2}{(1-t)^2 + 2(1-t)t\sigma} \tag{24}$$

Hence the difference between the linear GT and rational quadratic Bernstein bases is that of the changing speed of their parameters. Therefore

$$1 - \cos\theta = 1 - \cos\{\arctan \frac{\sqrt{2}(1-t)t + t^2}{(1-t)^2 + \sqrt{2}(1-t)t}\} = \frac{t^2}{(1-t)^2 + \sqrt{2}(1-t)t + t^2} \tag{25}$$

since $\cos(\arctan x) = 1/\sqrt{1+x^2}$. We have obtained the blending function for the third control points of the rational quadratic Bézier curve. Figure 7 shows $t - 2\{\arctan \frac{\sqrt{2}(1-t)t+t^2}{(1-t)^2+\sqrt{2}(1-t)t}\}/\pi$. Note that the value of

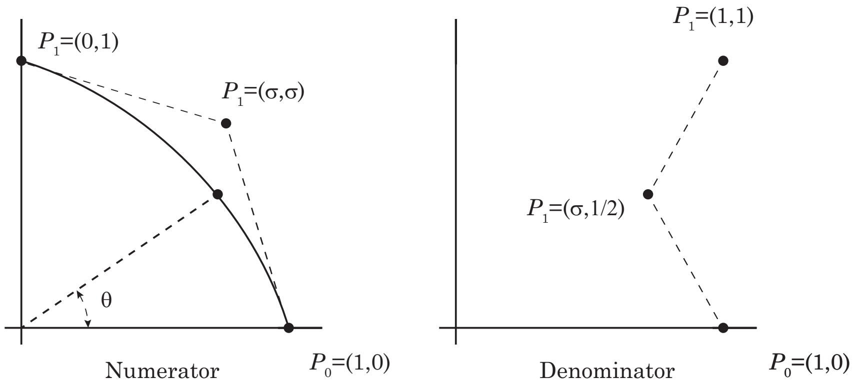

Figure 6: The numerator and denominator of the rational quadratic Bézier curve representing a quadrant of a unit circle

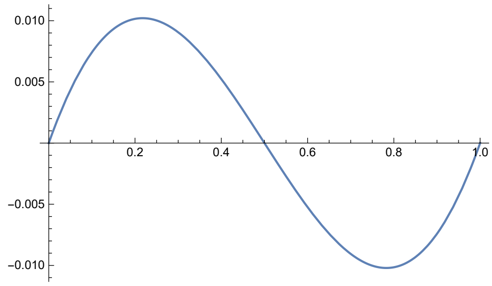

Figure 7: Parameter difference: $t - 2\{\arctan \frac{\sqrt{2}(1-t)t+t^2}{(1-t)^2+\sqrt{2}(1-t)t}\}/\pi$

$w(1/2)$ is determined by α, when $t = 1/2$, the parameter difference is 0.

Figure 8 shows the curvature distributions of a rational quadratic Bézier and linear GT curves defined by three control points $(0,0)$, $(2,0.5)$ and $(1,0)$. The weight of the Bézier curve is $1/\sqrt{2}$. Before reparameterization, the parameters at the peak of their curvature are different, but after reparameterization by Eq. (24), they become identical.

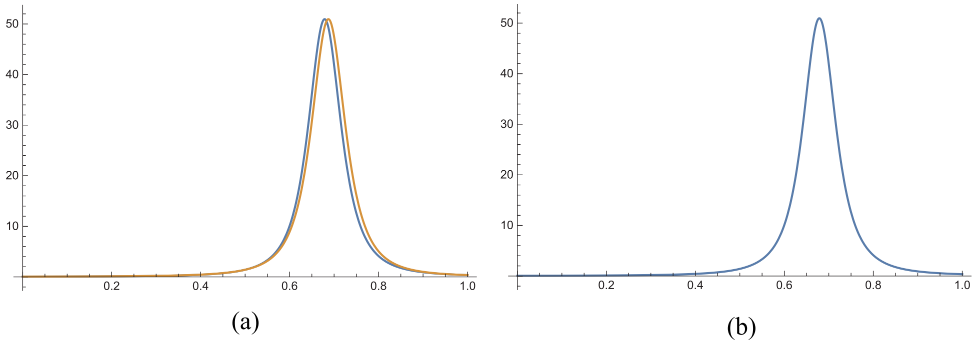

Figure 8: Curvature distribution (a) before reparameterization, (b) after reparameterization

7 COMPARISON BETWEEN LINEAR GH BASIS AND RATIONAL QUADRATIC BERNSTEIN BASIS

We would like to know how different are the linear GH and rational quadratic Bernstein bases. When $\boldsymbol{P}_0 = (\cosh(1)-1, -\sinh(1))$, $\boldsymbol{P}_1 = (0,0)$ and $\boldsymbol{P}_1 = (\cosh(1)-1, \sinh(1))$, the linear generalized hyperbolic curve with these control points becomes $(\cosh(2t-1)-1, \sinh(2t-1))$, i.e. hyperbola shown in Fig.9(a). For the same control points with $\sigma = (e+1)/(2\sqrt{e})$, the rational quadratic Bézier curve becomes the same hyperbola. Figure 9(b) compares the polar angles of the two curves. θ_H and θ_R are the polar angles of the linear GH and rational quadratic Bézier curves. Note that also in this case the value of $w(1/2)$ is determined by α, when $t = 1/2$, the parameter difference is 0.

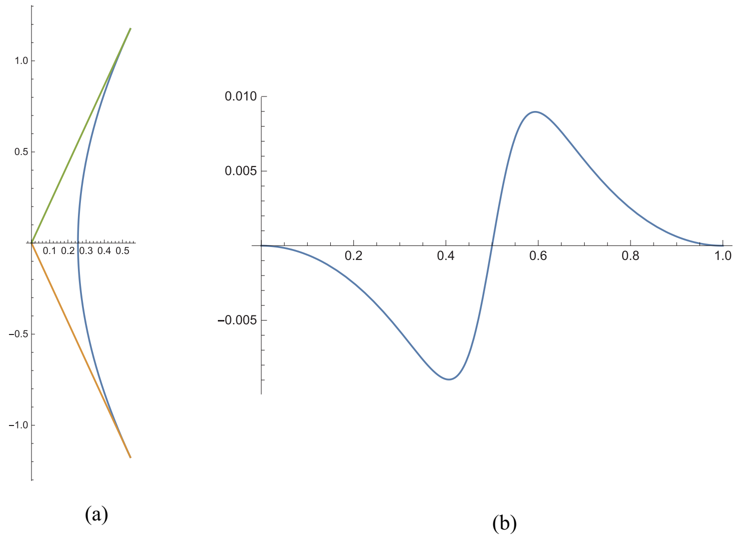

Figure 9: (a) Hyperbola, (b) Parameter difference: $\theta_H - \theta_R$

8 UNIQUENESS THEOREM OF THE SHAPE OF THE CURVE

We will prove a theorem called uniqueness theorem of the shape of the curve. We assume that for $0 \le t \le 1$ a curve $\boldsymbol{C}(t)$ is defined by three control points $\boldsymbol{P}_0$, $\boldsymbol{P}_1$ and $\boldsymbol{P}_2$ as

$$\boldsymbol{C}(t) = u(t)\boldsymbol{P}_0 + v(t)\boldsymbol{P}_1 + w(t)\boldsymbol{P}_2 \tag{26}$$

where $0 \le w(t) \le 1$, $0 \le v(t) \le 1$ and

$$\begin{aligned} u(t)+v(t)+w(t) &= 1 \\ u(t) &= w(1-t) \\ w(0) &= 0 \\ w(1) &= 1 \\ \frac{dw(t)}{dt} &> 0 \quad \text{for} \quad 0<t<1 \end{aligned} \tag{27}$$

If there is such a constant α that

$$v(t)^2 = \alpha u(t)w(t) \tag{28}$$

for $0 \le t \le 1$, then the following theorem is satisfied:

Theorem 1. *Uniqueness Theorem: The shape of the curve $\boldsymbol{C}(t)$ is determined by α exclusively and it does not depend on the basis functions $\{u(t), v(t), w(t)\}$ which are used to define the curve.*

Proof. For a given value $w_0 = w(t_0)$, $0 \le w_0 \le 1$, let $u_0 = u(t_0)$. Since $v(t) = 1 - u(t) - w(t)$,

$$(1-u_0-w_0)^2 = \alpha u_0 w_0 \tag{29}$$

Hence

$$u_0 = \frac{(\alpha-2)w_0 + 2 \pm \sqrt{\alpha w_0((\alpha-4)w_0+4)}}{2} \tag{30}$$

We assume u_0 is a continuous function of w_0 and $0 \le u_0 \le 1$ for $w_0 \in [0,1]$. Assume we select $+$ sign in the above expression, then $u_0 = 1$ when $w_0 = a$. Hence when $\alpha < 1$, u_0 can be less than 1. However when $\alpha < w_0 \le 1$, $u_0 > 1$. When $\alpha \ge 1$, $u_0 > 1$ for $w_0 \in (0,1)$. Therefore we should select $-$ sign in Eq.(30) and u_0 is uniquely determined. For any $\alpha > 0$, when w_0 is specified, we can determine parameter t_0 for the blending function $w(t)$ of the third control point of the rational quadratic Bézier curve with its weight σ such that $\alpha = 4\sigma^2$. We know the blending function $u(t)$ of the first control point of the curve and we obtain $u_0 = u(t_0)$. That means we have a unique solution of u_0 for any $\alpha > 0$.

Since u_0 is uniquely determined by w_0, the location of the point $\boldsymbol{C}(t_0)$ is also uniquely determined because $\{u(t), v(t), w(t)\}$ are barycentric coordinates of triangle $\boldsymbol{P}_0\boldsymbol{P}_1\boldsymbol{P}_2$. By changing t from 0 to 1, $w(t)$ also increases from 0 to 1 and the shape of the curve $\boldsymbol{C}(t)$ is also completely determined. □

Figure 10 shows u_0 for $0 \le w_0 \le 1$ and $0 \le \alpha \le 10$. Note that for these figures we change α until 10, but we will obtain similar figures for any $\alpha \ge 10$.

The final remark is that it is relatively easy to specify blending functions which have a property of partition of unity, but they do not satisfy Eq.(28). For example, $u(0) = 1 - \sqrt[3]{t}$, $w(t) = u(1-t)$, and $v(t) = 1 - u(t) - w(t)$. Then

$$\frac{v(t)^2}{u(t)w(t)} = \frac{\left(\sqrt[3]{1-t} + \sqrt[3]{t} - 1\right)^2}{\left(\sqrt[3]{1-t} - 1\right)\left(\sqrt[3]{t} - 1\right)} \tag{31}$$

Clearly the above expression is not a constant. The square of $\{u(t) + v(t) + w(t)\}^2$, for example, becomes a relatively complicated expression because there is no α such that $v(t)^2 = \alpha u(t)w(t)$.

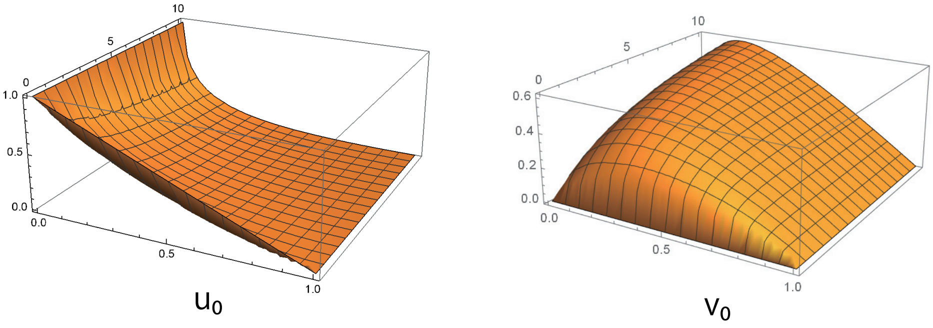

Figure 10: u_0 for $0 \leq w_0 \leq 1$ and $0 \leq \alpha \leq 10$

9 CONCLUSIONS

We have proved the uniqueness theorem on the shape of free-form curves defined by three control points, including non-rational and rational quadratic Bézier curves, generalized trigonometric and hyperbolic curves and splines in tension. We have also shown that we can generate infinite different Miura's triangles for different α values. For future work, we would like to extend our theorem for higher-degree free-from curves.

ACKNOWLEDGEMENTS

This work was supported by JST CREST Grant Number JPMJCR1911. It was also supported JSPS Grant-in-Aid for Scientific Research (B) Grant Number 19H02048, JSPS Grant-in-Aid for Challenging Exploratory Research Grant Number 26630038 Solutions and Foundation Integrated Research Program, and ImPACT Program of the Council for Science, Technology and Innovation. The authors acknowledge the support by 2016, 2018 and 2019 IMI Joint Use Program Short-term Joint Research "Differential Geometry and Discrete Differential Geometry for Industrial Design" (September 2016, September 2018 and September 2019). The third author acknowledges University Malaysia Terengganu.

Kenjiro T. Miura, http://orcid.org/0000-0001-9326-313
Dan Wang, http://orcid.org/0000-0003-1906-4998
R.U. Gobithaasan, http://orcid.org/0000-0003-3077-8772
Tadatoshi Sekine, http://orcid.org/0000-0003-1813-822X
Shin Usuki, http://orcid.org/0000-0003-1165-5507

REFERENCES

[1] Chelius, C.: Using the curvature tool in Adobe Illustrator, 2016. https://web.archive.org/web/20161023130701/https://creativepro.com/curvature-tool-adobe-illustrator/.

[2] Djudjic, D.: Photoshop CC officially gets curvature pen tool and other improvements, 2017. https://web.archive.org/web/20200620025914/https://www.diyphotography.net/photoshop-cc-officially-gets-curvature-pen-tool-improvements/.

[3] Erik Koch, P.; Lyche, T.: Construction of exponential tension b-splines of arbitrary order. In P.J. Laurent; A. Le Mehaute; L.L. Schumaker, eds., Curves and Surfaces, 255–258. Academic Press, 1991. ISBN 978-0-12-438660-0. http://doi.org/https://doi.org/10.1016/B978-0-12-438660-0.50039-X.

[4] Farin, G.: Curves and surfaces for CAGD. Morgan-Kaufmann, 2001.

[5] Miura, K.T.; Gobithaasan, R.U.; Wang, D.; Sekine, T.; Usuki, S.; Inoguchi, J.i.; Kajiwara, K.: $\epsilon\kappa$-curves: controlled local curvature extrema. The Visual Computer, 2021. http://doi.org/https://doi.org/10.1007/s00371-021-02149-8.

[6] Usman, M.M.; Abbas, M.; Miura, K.T.: Some engineering applications of new trigonometric cubic Bézier-like curves to free-form complex curve modeling. Journal of Advanced Mechanical Design, Systems, and Manufacturing, 14(4), 1, 2020. http://doi.org/10.1299/jamdsm.2020jamdsm0048.

[7] Yan, Z.; Schiller, S.; Schaefer, S.: Circle reproduction with interpolatory curves at local maximal curvature points. Computer Aided Geometric Design, 72(6), 98–110, 2019. http://doi.org/10.1016/j.cagd.2019.06.002.

[8] Yan, Z.; Schiller, S.; Wilensky, G.; Carr, N.; Schaefer, S.: κ-curves: Interpolation at local maximum curvature. ACM Transactions on Graphics, 36(4), Article 129, 2017. http://doi.org/10.1145/3072959.3073692.

Gobithaasan and Miura's Recursive Algorithm

For our new trigonometric basis, we can derive a recursive algorithm similar to de Casteljau's algorithm. For simplicity we explain only the quadratic case, but it can be extended to a general degree n by induction. To shorten expressions, we use $u = 1 - S(t)$, $v = S(t) + C(t) - 1$ and $w = 1 - C(t)$, where $S(t) = \sin\frac{\pi t}{2}$ and $C(t) = \cos\frac{\pi t}{2}$. Note that $v^2 = 2uw$, and

$$\begin{aligned}&(u+v+w)^2 = \\ &\quad u(u+v+w) + v(u+v+w) + w(u+v+w).\end{aligned} \tag{32}$$

For a quadratic curve with this basis, five control points P_i $(i = 0 \ldots 4)$ are used, and the curve point at t is evaluated as

$$\begin{bmatrix} u & v & w \end{bmatrix} \begin{bmatrix} P_0 & P_1 & P_2 \\ P_1 & P_2 & P_3 \\ P_2 & P_3 & P_4 \end{bmatrix} \begin{bmatrix} u & & \\ & v & \\ & & w \end{bmatrix}. \tag{33}$$

Hence the algorithm repeats a simple blending of three points $uP_{i-1} + vP_i + wP_{i+1}$ to generate a point on the given curve.

Miura's Triangle:

We can construct a triangle using the coefficients of trigonometric basis functions, similarly to Pascal's triangle. Below is a table of degree elevation, from the first row representing degree 1 to the sixth row representing degree 6:

$$\begin{array}{ccccccccccccc} & & & & & 1 & 1 & 1 & & & & & \\ & & & & 1 & 2 & 4 & 2 & 1 & & & & \\ & & & 1 & 3 & 9 & 8 & 9 & 3 & 1 & & & \\ & & 1 & 4 & 16 & 20 & 34 & 20 & 16 & 4 & 1 & & \\ & 1 & 5 & 25 & 40 & 90 & 74 & 90 & 40 & 25 & 5 & 1 & \\ 1 & 6 & 36 & 70 & 195 & 204 & 328 & 204 & 195 & 70 & 36 & 6 & 1 \end{array} \tag{34}$$

On how to construct Miura's triangle let's take a simple case from linear to quadratic. We use u, v and w to denote $u = 1 - S$, $v = S + C - 1$ and $w = 1 - C$. Then the following equation is satisfied:

$$v^2 = 2\,uw \tag{35}$$

Let's consider the following problem. We would like to know coefficients for the following expression:

$$(u + v + w)^n \tag{36}$$

When $n = 1$, we obtain

$$(u + v + w)^1 = c_{1,1}u + c_{1,2}v + c_{1,3}w \tag{37}$$

where of course $c_{1,1} = c_{1,2} = c_{1,3} = 1$. For $c_{i,j}$ the first suffix i indicates degree, i.e. the row of Miura's traingle and the second one j does the column of Miura's triangle. Then

$$\begin{aligned}
(u+v+w)^2 &= (u+v+w)u + (u+v+w)v + (u+v+w)w \\
&= \begin{array}{ccccccccc} u^2 & + & uv & + & uw & & & & \\ & + & uv & + & v^2 & + & vw & & \\ & & & + & uw & + & vw & + & w^2 \end{array} \\
&= \begin{array}{ccccccccc} u^2 & + & uv & + & uw & & & & \\ & + & uv & + & 2uw & + & vw & & \\ & & & + & uw & + & vw & + & w^2 \end{array}
\end{aligned} \tag{38}$$

Hence

$$\begin{aligned}
c_{2,1} &= c_{1,1} \\
c_{2,2} &= c_{1,2} + c_{1,1} \\
c_{2,3} &= c_{1,3} + 2\,c_{1,2} + c_{1,1} \\
c_{2,4} &= c_{1,2} + c_{1,1} \\
c_{2,5} &= c_{1,1}
\end{aligned} \tag{39}$$

Then we obtain the second row of Miura's triangle: $\{c_{2,1}, c_{2,2}, c_{2,3}, c_{2,4}, c_{2,5}\} = \{1, 2, 4, 2, 1\}$. We can repeat similar processes again and again and we can construct Miura's triangle.